DR AMANDA SCHRAGER-LAVELLE (Orcid ID : 0000-0003-2435-9336)

Article type : Original Article

Title

The Role of a Class III GA 2-Oxidase in Tomato Internode Elongation

Authors

Amanda Schrager-Lavelle, Natalie N. Gath, Upendra Kumar Devisetty, Esther Carrera, Isabel López-Díaz, Miguel A. Blazquez, and Julin N. Maloof

Addresses

Department of Plant Biology, University of California, Davis. One Shields Ave. Davis, California, 95616. (A.S-L., N.N.G., U.K.D., and J.N.M)

Instituto de Biología Molecular y Celular de Plantas (CSIC-Universidad Politécnica de Valencia), 46022 Valencia, Spain. (E.C., I.L-D., and M.A.B.)

Biology Department, Colorado Mesa University. 1100 North Ave. Grand Junction, Colorado, 81501. (Current address for A.S-L.)

Corresponding author

Julin N. Maloof

Department of Plant Biology, University of California, Davis, One Shields Ave. Davis, CA 95616

Phone: (530) 752-8077, Fax: (530) 752-5410, jnmaloof@ucdavis.edu

Email addresses

Amanda Schrager-Lavelle: alavelle@coloradomesa.edu

Natalie N. Gath: nngath@ucdavis.edu

Upendra Kumar Devisetty: upendrakumar.devisetty@googlemail.com

Esther Carrera: ecarrera@ibmcp.upv.es

Isabel López-Díaz: ilopez@ibmcp.upv.es

Miguel A. Blazquez: mblazquez@ibmcp.upv.es

Julin N. Maloof: jnmaloof@ucdavis.edu

Running title

The Role of a GA 2-oxidase in Tomato Internode Elongation

Key Words

Gibberellins, class III GA 2-oxidase, *Solanum lycopersicum*, tomato, internode elongation, bulked segregant analysis

Summary

A network of environmental inputs and internal signaling controls plant growth, development, and organ elongation. In particular, the growth promoting hormone gibberellin (GA) has been shown to play a significant role in organ elongation. Using tomato as a model organism to study elongation presents an opportunity to study the genetic control of internode specific elongation in a eudicot species with sympodial growth habit and substantial internodes that can and do respond to external stimuli. To investigate internode elongation, a mutant with an elongated hypocotyl and internodes but wild-type petioles was identified

through a forward genetic screen. In addition to stem specific elongation, this mutant, named *tomato internode elongated -1 (tie-1)* is more sensitive to the GA biosynthetic inhibitor paclobutrazol and has altered levels of intermediate and bioactive GAs as compared to wild-type plants. The mutation responsible for the internode elongation phenotype was mapped to *GA2oxidase 7*, a class III GA 2-oxidase in the GA biosynthetic pathway, through a bulked segregant analysis and bioinformatic pipeline, and confirmed by transgenic complementation. Furthermore, bacterially expressed recombinant TIE protein was shown to have *bona fide* GA 2-oxidase activity. These results define a critical role for this gene in internode elongation and are significant because they further the understanding of the role of GA biosynthetic genes in organ specific elongation.

Introduction

Plant growth and development is dependent not only on internal signals, but environmental factors. Internal factors such as hormone signaling, carbohydrate metabolism, and the circadian clock work in concert with environmental inputs such as light, biotic stresses, water and nutrient availability to control organ elongation in plants. While many of these pathways are well studied in Arabidopsis, flowering plants display great variation in their growth habits and architecture. Tomato, which has sympodial shoot development and substantial vegetative internodes, in particular has a different growth habit from the monopodial rosette architecture of the model plant Arabidopsis and model monocot rice (Kimura and Sinha, 2008). In addition, tomato is an agriculturally important crop and is closely related to many other crops including potato, eggplant, and pepper, together making tomato an excellent model for studying internode elongation, especially as conclusions drawn from studies done in tomato are more easily transferable to these closely related crop species.

A forward genetics approach is often used to identify novel genes involved in specific traits of interest. Once a mutant of interest is identified and characterized, bulked segregant analysis (BSA) is a powerful method for identifying the locus responsible for the mutant phenotype of interest (Michelmore et al., 1991). Traditional approaches to identifying a causative mutation or locus in the genome through BSA involve both recombinant genotyping and candidate gene sequencing; however, current high throughput genome sequencing techniques can be combined with these methods into a single, rapid step (Schneeberger et al., 2009). The advances in short read sequencing technology have allowed for the direct genome sequencing of mutant genomes to identify sites of mutation, however an ethane methyl sulfonate (EMS) mutagenized genome can possess hundreds or thousands of changes in addition to the causal mutation, making analysis and identification of the causal mutation difficult (Cuperus et al., 2010). BSA analysis combined with high throughput short read sequencing and a bioinformatics pipeline has been used successfully to identify causal loci in both plants (Chen et al., 2015; Cuperus et al., 2010) and animals (Bowen et al., 2012). Although internal signaling and external inputs work in concert to control elongation, there is a trade-off between the two. With respect to hormones, gibberellins (GA), auxin, ethylene, and brassinosteroids work through independent and overlapping signaling pathways to control elongation in plants (Lorrain and Fankhauser, 2012). Broadly, bioactive GAs modulate seed germination, flowering, and in particular, promote stem and leaf growth (Xu et al. 2014). The GA signal transduction pathway converts the GA signal into changes in gene expression and plant morphology. In both rice and Arabidopsis, these changes in gene expression occur through the GA INSENSITIVE DWARF 1 (GID1) GA receptors and GA dependent degradation of the DELLA transcriptional repressors (SLR1 in rice and the five member DELLA family in Arabidopsis) through the F-box protein homologs AtSLY1 and OsGID2 (Sun, 2011, Eckardt, 2007, and Sun and Gubler, 2004). As reviewed by Yamaguchi

(2008) and Xu et al. (2014), beyond the GA signal transduction pathway 136 structural variants of GA have been reported since the 1950's. While many forms of GA are found in plants, two GAs, GA_1 and GA_4, are the primary bioactive forms involved in modulating growth and development in most plants. This suggests that many of the remaining plant GAs are non-bioactive intermediates, precursors for bioactive GAs, or deactivated metabolites (Xu et al., 2014; Yamaguchi, 2008). In addition to the well-characterized GA biosynthetic pathway, the deactivation of bioactive GAs is also a critical component of GA regulation in plants. GA 2-oxidases are a gene family involved in the deactivation of bioactive GAs or in depleting pools of precursor GAs, with class I and class II GA 2-oxisases acting on 19C-GAs and class III GA 2-oxidasess acting on C_{20}-GAs (Schomburg et al., 2003; Yamaguchi, 2008). While the GA biosynthetic and signal transduction pathways are well described for Arabidopsis and rice, it is unknown how closely these model organisms reflect the pathways of other species that display very different morphologies.

To find genes not previously known to be important for shoot elongation in tomato, we took a forward genetics approach. Mutant lines with a constitutive elongation phenotype were screened for seedling hypocotyl length and adult internode and petioles lengths under long day white light conditions in a growth chamber. While many mutant lines displayed overall elongation in this initial screen, one mutant, named *tomato internode elongated -1 (tie-1),* was unusual in that it had an elongated hypocotyl and internodes, but wild-type petioles. This finding is significant not only because vegetative internodes are not easily assayed in Arabidopsis, but also because this mutant potentially provides a means to study internode elongation independent of petiole elongation. Here we describe characterization and cloning of the *tie-1* mutant.

Results

The *tomato internode elongated -1* mutant has an elongated hypocotyl and internodes but wild-type petioles

Several mutants were identified by an *in-silico* screen of the EMS and fast neutron mutagenized *Solanum lycopersicum cv M82* (M82) population. This population contained over 13,000 M2 families that were previously characterized for 15 primary and 48 secondary morphological categories (Menda et al., 2004). Mutants that were characterized in the primary category for growth habit and secondary category for elongation were selected. 10 of these mutant lines were further characterized for growth phenotypes including hypocotyl, internode, and petiole lengths. Among these mutant lines one EMS mutant (line e2265m1**)** stood out for stem specific elongation (Figure S1). This mutant, named *tomato internode elongated -1 (tie-1*; Figure 1A) was unique from the other lines screened in that it had an elongated hypocotyl (Figure 1B) and elongated internodes (Figure 1C and 1D), but wild-type petioles (Figure 1E and 1F) as compared to wild type M82. This suggests that the causative gene responsible for elongation in the *tie-1* mutant is specific for the control of elongation in the stem and does not play a significant role in petiole elongation. This mutant was chosen for further study because it presented an opportunity to investigate stem elongation as well as organ specific elongation.

tie-1 has a wild-type response to GA_3 application but is more sensitive than wild type to GA inhibition

The elongated internode phenotype of *tie-1* suggested that the phenotype might be caused by a mutation in a gene involved in growth control. The growth-promoting hormone GA was of particular interest because this hormone has previously been shown to play a significant role in organ elongation (Raskin and Kende, 1984, Ayano et al., 2014). To test whether *tie-1*

might have a defect in GA synthesis or response, the response of *tie-1* to both bioactive GA_3 and the GA biosynthetic inhibitor, paclobutrazol (PAC; Hedden and Graebe 1985), was assayed. Dose response curves for GA_3 application show that both internodes (Figure 2A) and petioles (Figure 2B) of the *tie-1* mutant and M82 show relatively similar elongation responses to GA_3 application ($p = 0.08 – 0.66$ for genotype differences in response to GA by linear regression; supplemental table 1). In contrast to the results of GA application, the dose response curve of PAC application show that the internodes of the *tie-1* mutant are significantly more sensitive to application of PAC (Figure 2C) than M82 ($p < 0.01$ for genotype differences in response to PAC by linear regression; supplemental table 1) while *tie-1* and M82 petioles (Figure 2D) are similarly inhibited by PAC application (p 0.1 – 0.5 for genotype differences in response to PAC by linear regression; supplemental table 1). The normal response of *tie-1* to GA suggests that the GA signaling pathway is unaffected by the *tie-1* mutation, whereas the increased resistance to PAC suggests that over-accumulation of GA could be responsible for the *tie-1* mutant phenotype.

Concentration of active and intermediate GAs are increased in the *tie-1* mutant

The response to PAC application suggested a defect in the GA biosynthetic pathway. To investigate this possibility, the *in-planta* concentration of different active and intermediate forms of GA were measured (Figure S2). Endogenous GA concentration of internode and petiole tissue was measured in three and a half week old *tie-1* and wild type plants. There was an overall increase in the bioactive GAs, GA_4 (Figure 3A) and GA_1, (Figure 3B) in the *tie-1* mutant. Interestingly, a largely internode specific increase in intermediates GA_{15} (Figure 3C) and GA_{44} (Figure 3D) was also noted. These results further implicate a mutation in the GA biosynthetic pathway as a cause of the hypocotyl and internode elongation in *tie-1*.

tie-1 heterozygotes display an intermediate phenotype

To identify the mutation responsible for the elongation phenotype, a mapping population was generated by outcrossing the *tie-1* mutant in the M82 background to *Solanum lycopersicum cv Heinz* (Heinz). Heinz was chosen due to availability of the sequenced genome (The Tomato Genome Consortium, 2012) and similar growth habit to that of M82 (Figure 4A). Any elongation observed in the progeny of the cross should be due to the *tie-1* mutation and not a contribution from either cultivar. Internode (Figure 4A) and petiole (Figure 4B) growth phenotypes of the heterozygous F1 plants were characterized. Interestingly, the internodes of the heterozygous F1 plants display an intermediate phenotype between the mutant *tie-1* parent and the Heinz parent. At five weeks of age, the internode 1 length of the F1 heterozygous plants were on average 50% longer than M82 but 18% shorter than the *tie-1* mutant, suggesting the causative mutation is either semi-dominant or haplo-insufficient. The petioles of the F1 heterozygous plants, as expected, are similar to that of both Heinz and the *tie-1* mutant parent, further suggesting the elongated internode phenotype of the F1 is due to the *tie-1* mutation and not an interaction between the M82 and Heinz cultivars.

Bulked segregant analysis reveals a mutation in a member of the *GA 2-Oxidase* gene family

BSA was used to map the mutation responsible for the internode elongation. To obtain a mutant pool, 1,000 F2 plants were visually phenotyped for internode elongation at three weeks of age. 23% of the F2 plants were identified as having the elongated internode homozygous *tie-1* phenotype. Based on a chi-square test ($P = 0.1441$), this result is not significantly different from the 25% expected for a single causative locus, suggesting that the *tie-1* phenotype is caused by a single locus. Genomic DNA from the phenotypically mutant F2 plants was pooled and sequenced using Illumina sequencing. The resulting sequence was

compared to M82 (Bolger et al. 2014) and Heinz (The Tomato Genome Consortium, 2012) genomic sequence to identify single nucleotide polymorphisms (SNPs) between M82, Heinz, and *tie-1*. It is expected that the genotype of the SNPs surrounding the *tie-1* locus will approach 100% M82/ 0% Heinz background in the mutant F2 pool due to the selection on the elongated-internode phenotype, and that there will be a novel polymorphism in *tie-1* not present in Heinz or M82.

The results of the BSA show a single peak on chromosome 2 where the segregation ratio reaches the 100% M82/ 0% Heinz expected of the causative locus. The remaining 11 chromosomes display the 50% M82/ 50% Heinz segregation ratio expected of unlinked loci (Figure 5). We conservatively defined the *tie1-1* candidate interval as the ~ 1.2 MB region where the average M82 SNP frequency was > 75%.

To further delineate possible candidate genes and the processes that *TIE1* might control, we performed RNAseq to compare the *tie1-1* and wild type M82 transcriptomes (Supplemental table 2). None of the top 10 downregulated genes (Table 1) are in the *tie-1* interval defined by BSA. Of the top up-regulated genes (Table 1) in the *tie1-1* interval there were several photosynthesis-related genes, whose up-regulation seems more likely to be a consequence rather than a cause of the *tie1-1* phenotype. Interestingly, the most strongly up-regulated gene is a GA 2-oxidase 2 homolog (located on chromosome 7) and the second-most strongly down-regulated gene codes for a homolog of the GA receptor like gene GID1L2 (located on chromosome 9). Although neither of these genes are in the *tie1-1* interval, their differential expression is consistent with *tie1-1* perturbing GA signaling as shown in Figures 2-3. Since the RNAseq did not point to obvious candidates for *tie1-1*, we next searched for mutations that would affect the protein sequence. While the identified region is gene dense and 1.2 Mb wide, only two genes in this region have a mutation that results in an amino acid sequence change and is near the expected 100% homozygosity at the locus of interest. A third gene in

the region has a silent mutation in the eighth exon of the coding sequence **(**Table 2**)**. One of these three genes, *GA 2-oxidase 7 (GA2ox7)* Solyc02g080120, has a single base change in the first intron at the first intron/second exon junction, leading to a splice site mutation and retention of the first intron. RNAseq analysis reveals retention of the first intron and an in-frame premature stop codon (Figure 6C, 6D, and 6E) in the *tie1-1* mutant, while the first intron of the *GA2ox7* is spliced out in M82 (Figure 6A, 6B, and 6E). In addition to the short read RNA sequencing, primers were designed to Sanger sequence the 5' end (spanning exon 1 and exon 2) of *GA2ox7* cDNA in M82 and *tie1-1*. The Sanger sequencing results confirm the *tie1-1* specific retention of intron 1 and the resulting in-frame premature stop codon in the *GA2ox7* mRNA. While a full-length transcript is made, it is presumed that the premature stop coding prevents translation of a functional protein. A loss of function mutation in this gene is consistent with the growth phenotypes, response to GA and PAC application, and perturbations to endogenous GA concentration observed in *tie1-1* mutants.

The second gene under the peak, an *ALPHA GLUCOSIDASE 1* belonging to Glycoside hydrolase family 31 (GH31AG) Solyc02g069670, has a single base change leading to a missense mutation (G696V) near the C-terminal end of the protein. While this amino acid change does have the potential to cause a significant change in protein function, the mutation is not in a previously characterized active site or conserved domain (Ernst et al., 2006) and is unlikely to explain the growth and GA phenotypes.

F2 mapping analysis eliminates GA31AG

The above analyses identified two candidate genes, *GH31AG (*Solyc02g069670*)* and *GA2ox7* (Solyc02g080120). To distinguish between these two candidates we performed a mapping experiment in which F2s from a *tie1-1* (M82 background) X Heinz cross were genotyped at both genes and phenotyped for internode elongation to test which of these genes was more

tightly linked to the phenotype. Multiple regression analysis showed that the mutant *ga2ox7* was strongly associated with increased elongation (P = 2.4e-11) whereas the mutant *gh31ag* was not (P = 0.8144). Combined with our other analyses, and the fact that these are the only mutant genes near the BSA interval, we conclude that the *tie1-1* phenotype is caused by the *ga2ox7* mutation.

The *tie1-1* phenotype is complemented by *GA2ox7*.

In order to confirm that *TIE1* is *GA2ox7,* complementation analysis was performed. *tie1-1* mutants complemented with the full length genomic sequence of *TIE1* under the control of the native promoter were assayed for epicotyl length and *TIE1* gene expression (Figure 7.) Consistent with *TIE1* being *GA2ox7*, complemented mutants do not display the *tie1-1* elongated internode phenotype ($P < 0.002$ for each of the rescue lines being shorter than *tie1-1)*. Interestingly, both rescue lines appeared even shorter than wild-type M82, and the degree of shortness correlated with the level of *TIE1* expression. However, the difference in epicotyl length between M82 and the rescue lines was not significant ($P > 0.3$). In summary, the transgenic complementation lines rescue the *tie1-1* mutant phenotype, confirming that the *tie1-1* mutant phenotype is due to disruption of *GA2ox7*, and it is possible that overexpression of *TIE1* would lead to plants shorter than wild type.

TIE1 shows GA 2-oxidase activity *in vitro*

To determine if TIE1 functions as a GA 2-oxidase, we expressed recombinant TIE1 in *E. coli* and assayed its activity on several C_{19} and C_{20} GA substrates. TIE1 resulted in the appearance of or increased levels of oxidized products while reducing the abundance of GA_{12}, GA_9, GA_{20}, and GA_1. In contrast, control extracts form *E. coli* not induced to produce TIE1

showed little or no activity (Figure 8). This demonstrates that TIE1 is a *bona fide* GA 2-oxidase and that it can work on both C_{20} and C_{19} substrates.

Discussion

This study describes a previously uncharacterized mutant in the tomato GA biosynthetic pathway and furthermore indicates that there is organ specificity in the control of GA mediated elongation. While the GA biosynthetic pathway in plants has been well studied, especially in Arabidopsis (Yamaguchi, 2008), studies of the intersection of GA biosynthesis and internode elongation done in Arabidopsis are limited due to the rosette structure and lack of substantial, measurable vegetative internodes. Tomato, on the other hand, is an excellent model for studying the control of internode elongation, as tomato has internodes that are highly responsive to external stimuli and internal signaling as seen with the transcription factor SlDREB which down-regulates GA biosynthesis in response to abiotic stresses resulting in shortened internodes (Li et al., 2012).

Bulked segregant analysis reveals the causative mutation in the *tie1-1* mutant.

Bulked segregant analysis is useful for finding the causative SNP, insertion/deletion (indel), or mutation affecting a phenotype or trait of interest. Combined with short read sequencing and bioinformatics approaches, BSA was used as a relatively fast way to map the causative mutation in the *tie1-1* mutant with just one generation of recombination. Although the region of chromosome 2 the *tie1-1* mutation mapped to is fairly large and gene rich, the list of candidate genes was limited. Only genes in the candidate region with base pair changes in the coding sequence at or near 100% homozygosity were considered. In the end, the list of candidates contained just two genes.

The first candidate gene coded for an ALPHA GLUCOSIDASE 1 (Solyc02g069670) belonging to Glycoside hydrolase family 31 (GH31AG), which contained a single base pair change in the *tie1-1* mutant that resulted in a missense mutation (G696V) near the C-terminus of the protein. As reviewed by Ernst et al. (2006), the GH31AG gene family is found across all domains of life and consists of four subgroups characterized by amino acid sequence (subgroups 1-4), with all plant GH31AGs belonging to subgroup 1. In addition, structural analysis of the GH31AG gene family has shown GH31AGs to be multi-domain proteins with four highly conserved domains. The N-terminal domain, Domain N, appears to contains residues essential for substrate binding and active site maintenance and architecture through interaction with catalytic site containing Domain A. The characteristic active site amino acid sequence of subtype 1 GH31AGs, WIDMNE, is involved in substrate binding. There is also a conserved C terminal domain with a currently unknown function (Ernst et al., 2006). While the G696V mutation in GH31AG is in a region of sequence conservation and has the potential to disrupt protein function, the mutation is not located in one of the four characterized conserved domains nor is it located in or near the characteristic active site. This, taken together with no correlation seen between the GH31AG mutation and elongation phenotype, means it is unlikely that the mutation in GH31AG is responsible for the elongation seen in the *tie1-1* mutant.

The second candidate gene, coding for *GA2ox7* (Solyc02g080120) contains a single base pair change in the *tie1-1* mutant which disrupts the canonical splice site acceptor sequence (GT-AG to GT-AT, Burset et al., 2000) at the last base of the first intron, leading to a retained first intron containing an in-frame stop codon. This mutation most likely prevents the translation of a functional protein, as no correctly spliced *GA2ox7* mRNA was found in the *tie1-1* mutant, while the majority of transcripts were as expected in wild-type M82.

Arabidopsis GA2ox 7 and 8 genes belong to a class of GA 2-oxidases, termed class III (Schomburg et al., 2003). Genes belonging to this class of 2-oxidases inactivate C_{20}-GA precursors (Figure S3) and can also act on C_{19} GAs (Pimenta Lange et al., 2013). Like the previously characterized class III GA 2-oxidases, *in-vitro* analysis shows a significant reduction in C_{20} GA_{12} and an increase in putative GA_{110} upon induction of TIE1. Although no standard is available for GA_{110} to positively confirm the compound generated, observed results are consistent with it being $GA_{110.}$ Like other class III GA 2-oxidases, TIE1 shows activity for C_{20} GAs and, interestingly, can also act on C_{19} GAs (Figure 8). The activity on C_{20} GAs is significant as these class III GA 2-oxidases are likely to play a role in depleting pools of precursor GAs (such as GA_{12} and GA_{53}) that are otherwise converted to bioactive forms (Yamaguchi, 2008). The increase in the intermediates GA_{15} and GA_{44} in *tie1-1* is consistent with the role of the class III GA 2-oxidases in GA biosynthesis, as these intermediates represent the next step in the pathway towards bioactive GA_1 and GA_4 when GA_{12} and GA_{53} (Supplemental figure 3) are not able to be converted into an inactive intermediate by GA2ox7. Additionally, the endogenous concentration of various active and intermediate GAs (figure 3 and supplemental figure 2) are generally higher in *tie1-1* internodes than M82 internodes. Although this trend does not hold true for every GA, we hypothesize that the difference in internode and petiole growth in *tie1-1* mutants is due in part to different affinities of GA receptors for bioactive GAs as has been demonstrated in rice (Ueguchi-Tanaka *et al.*, 2007) or indirect activation or induction of other GA2 oxidases due to the concomitant changes in endogenous GA levels. We hypothesize this alteration in the inactivation of early GA intermediates is responsible for the concomitant alterations in the accumulation of downstream intermediates and bioactive GAs.

tie1-1 growth phenotypes are organ specific and consistent with growth phenotypes of Arabidopsis _Atga2ox7_ and _Atga2ox8_ mutants

While the organ specific nature of GA biosynthesis and signal transduction is not well studied, organ specificity is not without precedence. In pea, differential expression of a GA catabolic gene, *PsGA2ox1*, between internode and tendril petioles suggests this gene plays a more important role in maintaining GA homeostasis in internodes than tendril petioles (Reinecke et al., 2013). Consistent with our finding that a loss of function *tie1-1* mutation in *SlGA2ox 7* results in an elongated phenotype, previous work done by Schomburg et al. (2003) on Arabidopsis class III GA 2-oxidase orthologs *AtGA2ox7* (*AT1G50960*) and *AtGA2ox8* (*AT4G21200*) showed that hypocotyls of *Atga2ox7* and *Atga2ox8* single and double mutants show significant elongation and that the phenotype of the double mutant was more elongated than either single mutant. Additionally, Schomberg et al. showed that overexpression of *AtGA2ox7* through activation tagging resulted in a shorter hypocotyl as compared to wild type (Schomburg et al., 2003). Like Arabidopsis, tomato also has two class III GA 2-oxidase orthologs, *Solyc10g005360* and the *tie1-1* gene *Solyc02g080120*. Although the loss of function phenotype of *Solyc10g005360* is unknown, the expression patterns of the tomato *GA2ox7* and *8* are suggestive of organ specificity with *Solyc02g080120* expressed higher in the internodes than petioles and *Solyc10g005360* not expressed in internodes (http://bar.utoronto.ca/efp_tomato/cgi-bin/efpWeb.cgi, Winter et al, 2007, Koenig et al. 2013). The organ specific phenotype of a loss of function mutation in *Solyc02g080120* presents an avenue for organ specific control of organ elongation through the GA biosynthetic pathway.

This study furthers the current understanding of *GA2ox7* by demonstrating organ specificity of these genes in the control of elongation in plants. Taken together, *tie1-1* endogenous GA concentrations that are consistent with a loss of function mutation in a class III GA 2-oxidase, the growth responses to GA and PAC application, and the BSA analysis and F2 mapping, *SlGA2ox7* Solyc02g080120 is likely a gene that inactivates C_{20}-GA precursors, thereby altering the landscape of inactive, precursor, and active GAs in tomato internodes and playing a significant role in the control of elongation in both hypocotyls and internodes.

Experimental procedures

Plant materials

The *tie1-1* mutant line (e2265m1) is an EMS mutant in the M82 background. Seed was obtained from the EMS and fast neutron mutagenized M82 population (http://zamir.sgn.cornell.edu/mutants) generated and maintained by the Zamir lab at the Hebrew University of Jerusalem. Wild-type cultivars M82 (accession LA3475) and Heinz (accession LA1706) seed were obtained from the UC Davis/C.M. Rick Tomato Genetics Resource Center.

Growth experiments

Hypocotyl

Seeds were surface sterilized with 50% household bleach and plated on 0.5x MSMO (Sigma-Aldrich) with 0.7% phytagar (Sigma-Aldrich,) in Phytatrays (Sigma-Aldrich). Plated seeds were kept in the dark for two days, then placed under white light in a growth chamber for one day. Seeds were then scored for germination to ensure only seeds with synchronized germination were used. The germinated seedlings remained under white light for an additional seven days. At 10 days post plating, seedlings with synchronized germination were

collected onto transparencies, scanned, and hypocotyl lengths measured from the scanned images using ImageJ (Schneider et al. 2012).

Internode and petiole

Seeds were surfaced sterilized with 50% household bleach and plated on moist paper towels in Phytatrays (Sigma-Aldrich). Plated seeds were kept in the dark for two days and then placed under white light for five days. One week after plating, uniform seedlings were transplanted to soil (commercial Sunshine Mix No. 1, Sun Gro Horticulture) in four-inch pots in a randomized block design and returned to the growth chamber. At three, four, and five weeks after plating, the epicotyl and first three internodes and first four petioles were measured with digital calipers (Mitutoyo) to capture organ length and growth rate over time.

GA_3 and paclobutrazol dose response

Seeds were plated, transplanted, and measured as described for internode and petiole measurements above. For the GA dose response, plants were sprayed with 0 μM (mock), 3 μM, or 10 μM GA_3 (Sigma-Aldrich) every second day beginning two weeks after plating. For the paclobutrazol (PAC) dose response, plants were watered with 5mL 0 μM (mock), 0.001 μM, 0.003 μM, 0.01 μM, 0.03 μM, or 0.1 μM PAC (Fluka) every third day beginning two and a half weeks after plating. Four weeks after plating, the epicotyl and first three internodes and first four petioles were measured with digital calipers to capture organ length. Statistical analysis was performed in R (R Core Team, 2014) using linear regression and plotted with ggplot2 (Wickham, 2016). Scripts available at https://github.com/MaloofLab/Lavelle-2018.

Endogenous GA concentration

Seeds were plated and transplanted as described for the internode and petiole measurements. 26 days after plating, internode 1 and petiole 2 tissue was collected into three biological replicates for each genotype. Each biological replicate contained 100-200 mg tissue fresh weight from 9 plants for both internode 1 and petiole 2. Tissue was flash frozen in liquid nitrogen, ground, and lyophilized for 48 hours. As previously described by Andres et al. (2014), the separated GAs were analyzed by electrospray ionization and targeted selected ion monitoring using a Q-Exactive spectrometer (Orbitrap detector; ThermoFisher Scientific). The [17,17-^{2}H] GAs were added to the extracts as internal standards for quantification, and the concentrations of GAs were determined using embedded calibration curves and the Xcalibur program 2.2 SP1 build 48.

Mapping population generation and screening

An F2 mapping population was generated by crossing the *tie1-1* mutant (in the M82 background) with the Heinz cultivar to generate heterozygous F1 seeds. Several F1 seeds were then planted and allowed to self-pollinate to generate the segregating F2 population. 1,000 F2 plants (in two rounds of 500 plants) were plated, transplanted, and grown as described in internode and petiole measurements above. The F2 population was then visually phenotyped for internode elongation at three weeks of age. Tissue from young leaves was collected using a leaf punch from each of the 230 positive plants. The tissue was pooled into groups of 10 and DNA was extracted using the Qiagen DNeasy kit. This DNA was combined into a single pool and used to make one unbarcoded library for high-throughput sequencing using the library construction protocol described in (Tsai et al., 2011). The library was sequenced in one lane of an Illumina Hi-Seq 2000 sequencer at the QB3 facility at UC Berkeley.

Bulked segregant analysis

Quality filtered *tie1-1* F2 BSA fastq reads (this study, M82 reads (Bolger et al., 2014), and Heinz reads (NCBI accession SRR404081) were mapped to the *Solanum lycopersicum* genome, release 2.40 (http://solgenomics.net/organism/Solanum_lycopersicum/genome; (Tomato Genome Consortium, 2012)) using BWA (Li and Durbin, 2009). Duplicate reads were removed using Samtools (Li et al., 2009). Polymorphisms were identified using freebayes v0.9.21-19-gc003c1e (Garrison and Marth, 2012). SNP effects were determined using SnpEFF (Cingolani et al., 2012). Downstream analysis, SNP filtering, and plotting were performed in R (R Core Team, 2014). In this downstream analysis, SNPs were filtered to keep those with a read depth between 5 and 149 (*tie1-1* F2s) or between 5 and 199 (M82 and Heinz). For determining SNP frequency in the *tie1-1* F2s we only considered SNPs where M82 differed from Heinz. For the details of our analysis and accompanying R scripts please see https://github.com/MaloofLab/Lavelle-2018.

RNA sequencing sample preparation and sequencing

tie1-1 and M82 seeds were plated and transplanted as described for the internode and petiole measurements. Three weeks after plating, epicotyl tissue was collected into three biological replicates for each genotype. Each biological replicate contained tissue from three plants. Tissue was flash frozen in liquid nitrogen and RNA was extracted using a Qiagen RNeasy kit, including an on-column DNase treatment (Qiagen).

The quality and quantity of the extracted RNA was initially assessed by NanoDrop ND 1000 (NanoDrop technologies). RNA-Seq libraries were prepared from 6 samples using Illumina's TruSeq^{TM} v1 RNA sample Preparation kit (RS-930-2002) with a Low-Throughput protocol following manufacturer's instructions with few modifications as described (Devisetty et al., 2014). The six libraries, along with 92 libraries from a different experiment, were then

quantified on an Analyst Plate Reader (LJL Biosystems) using SYBR Green I reagent (Invitrogen). These 96 library samples were then pooled in equimolar ratios to a final concentration of 20 nM and sequenced using an Illumina HiSeq2000 (50-bp, single-end reads) at the QB3 facility at UC Berkeley.

The FastX-tool kit software (http://hannonlab.cshl.edu/fastx_toolkit/) and custom perl scripts were used to perform pre-processing of Illumina raw reads to ensure the good quality of sequencing reads for downstream analysis. The raw reads were either quality filtered with fastq_quality_filter with parameters [-q 20, -p 95] or in some cases trimmed using fastx_trimmer with parameters [-f 9; -l 50]. Next, reads containing custom adapters were removed using a custom script. The reads were then sorted (de-multiplexed) by their custom barcode sequences using a custom script (https://github.com/mfcovington/auto_barcode). Reads were checked for quality before and after quality control with FastQC quality assessment software (http://www.bioinformatics.babraham.ac.uk /projects/fastqc/).

Differential expression and intron retention analysis

tie1-1 and M82 RNA sequences were mapped to the *Solanum lycopersicum* genome, release 2.40 (http://solgenomics.net/organism/Solanum_lycopersicum/genome; (Tomato Genome Consortium, 2012)) using Tophat2 (Trapnell et al., 2012; Trapnell et al., 2009). To determine the proportion of correctly or incorrectly spliced transcripts in *tie1-1* and M82, reads were visualized using the Integrative Genome Viewer (IGV; Thorvaldsdóttir et al., 2013; Robinson et al., 2011) and manually counted.

To look for differentially expressed genes, RNAseq reads were mapped to the ITAG2.3 cDNA reference sequences ((Tomato Genome Consortium, 2012) using BWA (Li and Durbin, 2009). Read counts were normalized using the trimmed mean of m-values (TMM)

method (Robinson and Oshlack, 2010) and differential expressed genes were determined using edgeR (Robinson et al., 2010).

Complementation analysis

Full-length genomic sequence of wild type M82-derived Solyc02g080120, including approximately 4,800bp upstream and 700bp downstream, was cloned into expression vector pMDC99. The pMDC99 vector contains a 35S:HPT hygromycin resistance gene for plant selection (Curtis and Grossniklaus, 2003). The pMDC99 vector containing the Solyc02g080120 genomic clone was transformed into Agrobacterium strain GV3101 via heat shock transformation. Transgenic lines were generated through Agrobacterium mediated tissue culture transformation by The Ralph M. Parsons Foundation Plant Transformation Facility, University of California, Davis, One Shields Ave, Davis, CA 95616 using a protocol modified from Fillatti et al. (1987). Transformants were propagated in the UC Davis College of Biological Sciences Orchard Park Greenhouse Facility. Plants were grown as described above.

***In-vitro* TIE1 activity assay**

The coding region of the M82 Solyc02g080120 was cloned into pCR8/GW/TOPO (Invitrogen) and mobilized to the pDEST17 vector (Invitrogen) for expression in Rosetta *E. coli* cells. Induction of TIE1-6xHis tagged protein was achieved by incubation with IPTG 0.5 mM for 2 hours at 37ºC. Cell lysates were prepared by suspending initial 25 mL pelleted cultures in TrisHCl 1 mL pH 7.5, DTT 4 mM and lysozyme 1 mg/mL. Samples were incubated at room temperature for 15 minutes and sonicated on ice 3 times for 3 seconds each. Extracts were centrifuged at 10,000 rpm for 5 min at 4ºC. Enzymatic assay of GA2ox7 activity was performed on freshly prepared cell lysates. 90 µL aliquots of lysates were incubated at 30ºC for 2 h at 50rpm with either [17-$^2H_2$]-GA9, [17-$^2H_2$]-GA4, [17-$^2H_2$]-GA20, [17-$^2H_2$]-GA1, [17-$^2H_2$]-GA12 or [17-$^2H_2$]-GA53 in a total volume of 100 µL containing 2-

oxoglutarate 4 mM, ascorbate 4 mM, ferrous sulphate 0.5 mM, DTT 4 mM and BSA 2 mg/mL. The [17-$^{2}H_2$]-GAs, deuterium-labeled gibberellins, were purchased from OlChemim Ltd (Olomouc, Czech Republic.)

The reaction mixture was dried in a vacuum evaporator, suspended in 80% methanol-1% acetic acid and mixed by shaking for one hour at 4ºC. The extract was kept at -20ºC overnight then centrifuged and the supernatant dried in a vacuum evaporator. The dry residue was dissolved in 1% acetic acid and passed through a reverse phase column (HLB Oasis 30 mg, Waters), as described in Seo et al. (2011). The eluted residues were dried and dissolved in 5% acetonitrile-1% acetic acid and the gibberellin metabolites were separated by UHPLC with a Accucore C18 reverse column (2.6 µm, 100 mm length; Thermo Fisher Scientific) with a 2 to 55% acetonitrile gradient containing 0.05% acetic acid, at 400 µL/min over 21 min. The metabolites were analyzed with a Q-Exactive mass spectrometer (Orbitrap detector; ThermoFisher Scientific) by targeted Selected Ion Monitoring (tSIM; capillary temperature 300ºC, S-lens RF level 70, resolution 70.000) and electrospray ionization (spray voltage 3.0 kV, heater temperature 150ºC, sheath gas flow rate 40 µL/min, auxiliary gas flow rate 10 µL/min) in negative mode. The presence of the different gibberellin peaks in the lysates was identified by the Xcalibur 4.0 and TraceFinder 4.1 SP1 programs.

Accession numbers

Sequencing reads from the F2 bulk segregant analysis as well as *tie1-1* and M82 RNA sequencing are available as NCBI Bioproject PRJNA494243 (https://www.ncbi.nlm.nih.gov/bioproject/PRJNA494243).

Acknowledgements

This work used the Vincent J. Coates Genomics Sequencing Laboratory at UC Berkeley, supported by NIH S10 Instrumentation Grants S10RR029668 and S10RR027303. We thank the Tomato Genetics Resource Center for providing seed of the M82 and Heinz cultivars. The MATERIAL was developed by and/or obtained from the UC Davis/C.M. Rick Tomato Genetics Resource Center and maintained by the Department of Plant Sciences, University of California, Davis, CA 95616. We thank Anthony Bolger, Alisdair Fernie, and Björn Usadel for providing us access to pre-publication genomic reads of the *S. lycopersicum* cultivar M82, and Cristina Úrbez and Noel Blanco-Touriñán (IBMCP, Spain) for technical help with *in vitro* production of TIE1. This work was supported in part by the Elsie Taylor Stocking Memorial Fellowship awarded to A.S.L. in 2013, by NSF grant IOS-0820854, by USDA National Institute of Food and Agriculture project CA-D-PLB-2465-H, by internal UC Davis funds, and by Spanish Ministry of Economy and Competitiveness grant BFU2016-80621-P.

Conflict of Interest

The authors declare no conflict of interest associated with the work described in this manuscript.

Legends for supporting information

Supplemental figure 1: Mutant screen.

Supplemental figure 2: Endogenous GAs measured in *tie1-1* and M82 internodes and petioles.

Supplemental figure 3: GA biosynthetic pathway.

Supplemental table 1: Stats from linear regression analysis of dose response assays.

Supplemental table 2: All differentially expressed genes between M82 and tie1-1.

References

Andrés, F., Porri, A., Torti, S., Mateos, J., Romera-Branchat, M., García-Martínez, J.L., Fornara, F., Gregis, V., Kater, M.M., and Coupland, G. (2014) SHORT VEGETATIVE PHASE reduces gibberellin biosynthesis at the Arabidopsis shoot apex to regulate the floral transition. Proc. Natl Acad. Sci. USA, *111*, E2760-E2769.

Ayano, M., Kani, T., Kojima, M., Sakakibara, H., Kitaoka, T., Kuroha, T., Angeles-Shim, R.B., Kitano, H., Nagai, K., and Ashikari, M. (2014) Gibberellin biosynthesis and signal transduction is essential for internode elongation in deepwater rice. Plant, Cell, Environ. *37*, 2313-2324.

Bolger, A., Scossa, F., Bolger, M.E., Lanz, C., Maumus, F., Tohge, T., Quesneville, H., Alseekh, S., Sørensen, I., Lichtenstein, G., et al. (2014) The genome of the stress-tolerant wild tomato species Solanum pennellii. Nat. Genet., 46, 1034–1038.

Bowen, M.E., Henke, K., Siegfried, K.R., Warman, M.L., and Harris, M.P. (2012) Efficient mapping and cloning of mutations in zebrafish by low-coverage whole-genome sequencing. Genetics, *190*, 1017-1024.

Burset, M., Seledtsov, I.A., and Solovyev, V.V. (2000) Analysis of canonical and non-canonical splice sites in mammalian genomes. Nucleic Acids Res., *28*, 4364-4375.

Chen, W., Yao, J., Chu, L., Yuan, Z., Li, Y., and Zhang, Y. (2015) Genetic mapping of the nulliplex-branch gene (gb_nb1) in cotton using next-generation sequencing. Theor. Appl. Genet., *128*, 539-547.

Cingolani, P., Platts, A., Wang, L.L., Coon, M., Nguyen, T., Wang, L., Land, S.J., Lu, X., and Ruden, D.M. (2012) A program for annotating and predicting the effects of single nucleotide polymorphisms, SnpEff: SNPs in the genome of Drosophila melanogaster strain w1118; iso-2; iso-3. Fly, 6, 80–92.

Cuperus, J.T., Montgomery, T.A., Fahlgren, N., Burke, R.T., Townsend, T., Sullivan, C.M., and Carrington, J.C. (2010) Identification of MIR390a precursor processing-defective mutants in Arabidopsis by direct genome sequencing. Proc. Natl Acad. Sci. USA, *107*, 466-471.

Curtis, M. D. & Grossniklaus, U. (2003) A gateway cloning vector set for high-throughput functional analysis of genes *in planta*. Plant Physiol. **133**, 462-469, doi:10.1104/pp.103.027979.

Devisetty UK, Covington MF, Tat AV, Lekkala S, Maloof JN (2014) Polymorphism identification and improved genome annotation of *Brassica rapa* through deep RNA sequencing. G3 (Bethesda), 4, 2065-2078

Eckardt, N.A. (2007) GA Perception and Signal Transduction: Molecular Interactions of the GA Receptor GID1 with GA and the DELLA Protein SLR1 in Rice. Plant Cell, 19, 2095-2097.

Ernst, H.A., Lo Leggio, L., Willemoës, M., Leonard, G., Blum, P., and Larsen, S. (2006) Structure of the *Sulfolobus solfataricu*s α-Glucosidase: Implications for domain conservation and substrate recognition in GH31. J. of Mol. Biol., *358*, 1106-1124.

Fillatti, J. J., Kiser, J., Rose, R. & Comai, L. (1987) Efficient transfer of a glyphosate tolerance gene into tomato using a binary *Agrobacterium Tumefaciens* vector. Nat Biotech **5**, 726-730.

Hedden, P., and Graebe, J.E. (1985) Inhibition of gibberellin biosynthesis by paclobutrazol in cell-free homogenates of *Cuburbita maxima* endosperm and *Malus pumia* embryos. J Plant Growth Regul, *4*, 111-122.

Garrison E, Marth G. (2012) Haplotype-based variant detection from short-read sequencing. arXiv preprint arXiv:1207.3907 [q-bio.GN].

Kimura, S., and Sinha, N. (2008) Tomato (*Solanum lycopersicum*): A model fruit-bearing crop. Cold Spring Harbor Protocols, pdb.emo105.

Koenig, D., Jiménez-Gómez, J.M., Kimura, S., Fulop, D., Chitwood, D.H., Headland, L.R., Kumar, R., Covington, M.F., Devisetty, U.K., Tat, A.V., Tohge, T., Bolger, A., Schneeberger, K., Ossowski, S., Lanz, C., Xiong, G., Taylor-Teeples, M., Brady, S.M., Pauly, M., Weigel, D., Usadel, B., Fernie, A.R., Peng, J., Sinha, N.R. and Maloof, J.N. (2013) Comparative transcriptomics reveals patterns of selection in domesticated and wild tomato. Proc. Natl Acad. Sci. USA 110, E2655.

Li, H., and Durbin, R. (2009) Fast and accurate short read alignment with Burrows–Wheeler transform. Bioinformatics, *25*, 1754-1760.

Li, H., Handsaker, B., Wysoker, A., Fennell, T., Ruan, J., Homer, N., Marth, G., Abecasis, G., and Durbin, R. (2009) The Sequence Alignment/Map format and SAMtools. Bioinformatics, 25, 2078–2079.

Li, J., Sima, W., Ouyang, B., Wang, T., Ziaf, K., Luo, Z., Liu, L., Li, H., Chen, M., Huang, Y., *et al.* (2012) Tomato SlDREB gene restricts leaf expansion and internode elongation by downregulating key genes for gibberellin biosynthesis. J.Exp. Bot., *63*, 6407-6420.

Lorrain, S., and Fankhauser, C. (2012) Plant Development: Should I stop or should I grow? Curr. Biol., *22*, R645-R647.

Menda, N., Semel, Y., Peled, D., Eshed, Y., and Zamir, D. (2004) In silico screening of a saturated mutation library of tomato. Plant J., *38*, 861-872.

Michelmore, R.W., Paran, I., and Kesseli, R.V. (1991) Identification of markers linked to disease-resistance genes by bulked segregant analysis: a rapid method to detect markers in specific genomic regions by using segregating populations. Proc. Natl Acad. Sci. USA, *88*, 9828-9832.

Pimenta Lange, M.J., Liebrandt, A., Arnold, L., Chmielewska, S.-M., Felsberger, A., Freier, E., Heuer, M., Zur, D. and Lange, T. (2013) Functional characterization of gibberellin oxidases from cucumber, Cucumis sativus L. Phytochemistry, 90, 62-69.

R Core Team (2014) R: A Language and environment for statistical computing.

Schneeberger, K., Ossowski, S., Lanz, C., Juul, T., Petersen, A.H., Nielsen, K.L., Jorgensen, J.-E.

Raskin, I., and Kende, H. (1984) Role of gibberellin in the growth response of submerged deep water rice. Plant Physiol., *76*, 947-950.

Reinecke, D.M., Wickramarathna, A.D., Ozga, J.A., Kurepin, L.V., Jin, A.L., Good, A.G., and Pharis, R.P. (2013) Gibberellin 3-oxidase gene expression patterns influence gibberellin biosynthesis, growth, and development in pea. Plant Physiol., *163*, 929-945.

Robinson MD, Oshlack A. (2010) A scaling normalization method for differential expression analysis of RNA-seq data. Genome biology. 11(3):R25.

Robinson, M.D., McCarthy, D.J., and Smyth, G.K. (2010) edgeR: a Bioconductor package for differential expression analysis of digital gene expression data. Bioinformatics, *26*, 139-140.

Robinson, J.T., Thorvaldsdóttir, H., Winckler, W., Guttman, M., Lander, E.S., Getz, G., and Mesirov, J.P. (2011) Integrative genomics viewer. Nat Biotech, 29, 24–26.

Schneeberger, K., Ossowski, S., Lanz, C., Juul, T., Petersen, A.H., Nielsen, K.L., Jorgensen, J.-E., Weigel, D., and Andersen, S.U. (2009) SHOREmap: simultaneous mapping and mutation identification by deep sequencing. Nat Meth, *6*, 550-551.

Schneider, C.A., Rasband, W.S., and Eliceiri, K.W. (2012) NIH Image to ImageJ: 25 years of image analysis. Nat Meth, *9*, 671-675.

Schomburg, F.M., Bizzell, C.M., Lee, D.J., Zeevaart, J.A.D., and Amasino, R.M. (2003) Overexpression of a novel class of gibberellin 2-oxidases decreases gibberellin levels and creates dwarf plants. Plant Cell, *15*, 151-163.

Seo, M., Jikumaru, Y., Kamiya, Y. (2011) Profiling of Hormones and Related Metabolites in Seed Dormancy and Germination Studies. Methods in Molecular Biology 773: 99-111

Sun, T.-p., and Gubler, F. (2004) Molecular mechanism of gibberellin signaling in plants. Annu. Rev. Plant Biol., *55*, 197-223.

Sun, T.-p. (2011) The Molecular Mechanism and Evolution of the GA–GID1–DELLA Signaling Module in Plants. Current Biology, *21*, R338-R345.

The Tomato Genome Consortium (2012) The tomato genome sequence provides insights into fleshy fruit evolution. Nature, *485*, 635-641.

Thorvaldsdóttir, H., Robinson, J.T., and Mesirov, J.P. (2013) Integrative Genomics Viewer (IGV): high-performance genomics data visualization and exploration. Brief Bioinform, 14, 178–192.

Trapnell, C., Pachter, L., and Salzberg, S.L. (2009) TopHat: discovering splice junctions with RNA-Seq. Bioinformatics, 25, 1105–1111.

Trapnell, C., Roberts, A., Goff, L., Pertea, G., Kim, D., Kelley, D.R., Pimentel, H., Salzberg, S.L., Rinn, J.L., and Pachter, L. (2012) Differential gene and transcript expression analysis of RNA-seq experiments with TopHat and Cufflinks. Nature Protocols, 7, 562–578.

Tsai, H., Howell, T., Nitcher, R., Missirian, V., Watson, B., Ngo, K.J., Lieberman, M., Fass, J., Uauy, C., Tran, R.K., *et al.* (2011) Discovery of rare mutations in populations: TILLING by sequencing. Plant Physiol., *156*, 1257-1268.

Ueguchi-Tanaka, M., Nakajima, M., Katoh, E., Ohmiya, H., Asano, K., Saji, S., Hongyu, X., Ashikari, M., Kitano, H., Yamaguchi, I. and Matsuoka, M. (2007) Molecular interactions of a soluble gibberellin receptor, GID1, with a rice DELLA protein, SLR1, and Gibberellin. Plant Cell, 19, 2140.

Wickham, H. (2016). ggplot2: elegant graphics for data analysis. Springer-Verlag New York.

Winter, D., Vinegar, B., Nahal, H., Ammar, R., Wilson, G.V. and Provart, N.J. (2007) An "Electronic Fluorescent Pictograph" Browser for Exploring and Analyzing Large-Scale Biological Data Sets. PLOS ONE, 2, e718.

Xu, H., Liu, Q., Yao, T., and Fu, X. (2014) Shedding light on integrative GA signaling. Curr. Opin. Plant Biol., *21*, 89-95.

Yamaguchi, S. (2008) Gibberellin metabolism and its regulation. Annu. Rev. Plant Biol., *59*, 225-251.

Figure legends

Figure 1. Growth phenotypes of *tie1-1* and M82.

Representative M82 (left) and *tie1*-1 (right) plants (a). Hypocotyl length (b) of 10 day old *tie1-1* and M82 seedlings grown on 0.5x MSMO and 0.7% agar in Phytatrays under long day (16:8) white light conditions in a growth chamber. n = >30 for each genotype. Length of epicotyl (c), internode 1 (d), petiole 1 (e), and petiole 2 (f) of three, four, and five week old *tie1-1* and M82 plants grown on soil in four-inch pots under long day (16:8) white light in a growth chamber. n = 8 for each genotype. The error bars show +/- SE.

Figure 2. Response to application of bioactive GA_3 and GA biosynthetic inhibitor PAC.

Internode length (a) and petiole length (b) of GA_3 treated *tie1-1* and M82 plants grown in 4-in pots in soil under long day white light conditions in a growth chamber. Plants were sprayed with 0 μM (mock), 3 μM, or 10 μM GA_3 every two days beginning two weeks after plating. Internode length (c) and petiole length (d) of PAC treated *tie1-1* and M82 plants grown in 4-in pots in soil under long day white light conditions in a growth chamber. Plants were watered with 0 μM (mock), 0.001 μM, 0.003 μM, 0.01 μM, 0.03 μM, or 0.1 μM every three days beginning two and a half weeks after plating. Measurements for both treatments were taken four weeks after plating and n = 8 for each genotype, treatment, and concentration. Error bars represent +/- SE.

Figure 3. Endogenous concentration of various active and intermediate and GAs.

Endogenous concentration of active GA_4 (a) and GA_1 (b) and inactive intermediates GA_{15} (c) and GA_{44} (d) in the *tie1-1* mutant and M82 internodes and petioles. 100-200 mg FW was harvested from three and a half week old plants grown under long day white light conditions in a growth chamber. Nine plants contributed to each of three biological replicates for each

organ or each genotype. Error bars represent +/- SE. *** $p < 0.001$, ** $p < 0.01$, * $p < 0.05$, NS = not significant.

Figure 4. Growth phenotypes of the Heinz mapping parent, wildtype M82, *tie1-1* mutant, and F1 progeny of a Heinz x *tie1-1* cross.

Internode 1 length (a) and petiole 2 length (b) of three, four, and five week old Heinz mapping parent, wildtype M82, *tie1-1* mutant, and F1 generation of a Heinz x *tie1-1* cross plants grown on soil in four-inch pots under long day (16:8) white light in a growth chamber. n = 8 for each genotype. The error bars show +/- SE.

Figure 5. BSA reveals a peak on chromosome 2.

Each point represents a SNP segregating between M82 and Heinz in the *tie1-1* BSA pool. The y-axis indicates the percentage of reads that had the M82 genotype in the *tie1-1* BSA pool. The x-axis indicates the position along the chromosome in base pairs. The line shows a 20 SNP running average of M82 percentage.

Figure 6. Gene model of the M82 and *tie1-1 GA2ox7* and quantification of *tie1-1* intron retention.

(a) and (c): Schematic showing the wild-type and *tie1-1* gene structure (respectively) and the G->T splice acceptor base change. (b) and (d): Plot of M82 (b) and *tie1-1* (d) Illumina RNAseq reads mapped to the Heinz genome. Thin lines connect splice junctions present in the RNAseq reads and thick lines indicate alignment between an RNAseq read and the reference. Note the extensive retention of intron 1 in *tie1-1*. (e) Quantification of reads that are spliced or unspliced crossing the 5' or 3' intron 1 splice junction. The apparent intron splicing indicated by 6 reads in the *tie1-1* intron 1 (d) is actually due to read-misalignment by

the mapping software and upon detailed inspection these reads do not represent intron 1 splicing.

Figure 7. Full length *GA2ox7* (Solyc02g080120) complements the *tie1-1* phenotype. Gene expression of *GA2ox7* and epicotyl length of 4 week old M82, *tie1-1,* and two independent complementation lines. Plants were grown on soil in four-inch pots under long day (16:8) white light in a growth chamber. n > 5 for each genotype. The error bars show +/- SE.

Figure 8. TIE1 catalyzes the oxidation of C_{19}- and C_{20}-GA molecules.
(a) Schematic representation of GA metabolism highlighting the GA molecules analyzed in the in vitro activity tests. Shaded in blue are the oxidized compounds. Red arrows indicate the reactions catalyzed by 2-oxidases. (b) Coomasie-stained gel showing the production of TIE-6xHis in *E. coli*. (c) Use of different GA molecules (left column) and production of their oxidized versions (right column) by bacterial extracts containing TIE-6xHis induced or not induced at 37ºC for 2 h. Exp 1 and Exp 2 are two biological replicates using 5 and 10 ppb, respectively, of GA12, GA9, GA20 and GA1. The most likely ion diagnostic for GA110 is that of m/z = 349.19895, but there is no standard available.

Tables

Table 1. Differentially expressed genes between M82 and *tie1-1*.

Top 10 down-regulated genes.

ITAG	logFC	logCPM	LR	P-Value	FDR	ITAG gene annotation
Solyc03g116820	-8.209819914	1.634116934	397.391748	2.04E-88	4.40E-85	Phox domain-containing protein
Solyc09g075690	-7.422752634	3.265406682	292.0147645	1.81E-65	1.96E-62	Gibberellin receptor GID1L2
Solyc09g007940	-7.314886198	6.219489829	201.6440784	9.14E-46	4.32E-43	Adenosine kinase
Solyc11g030380	-7.085812314	2.46836931	399.775265	6.16E-89	1.55E-85	MADS box interactor-like
Solyc11g011980	-4.749064231	2.587296606	268.6742669	2.21E-60	2.09E-57	WD-40 repeat protein
Solyc11g021060	-4.45535011	3.357215578	408.2077309	9.00E-91	2.72E-87	Proteinase inhibitor
Solyc11g020980	-4.054274525	2.808475494	418.9347264	4.16E-93	1.57E-89	Unknown Protein
Solyc09g092670	-3.981224808	2.111634503	247.9705946	7.19E-56	4.73E-53	Cytochrome P450
Solyc03g034380	-3.94647864	4.456281835	169.446655	9.77E-39	3.61E-36	Lipid transfer protein
Solyc03g114530	-3.78248247	3.865328381	206.2693362	8.95E-47	4.67E-44	Strictosidine synthase family protein

Top 10 up-regulated genes.

ITAG	logFC	logCPM	LR	P-Value	FDR	ITAG gene annotation
Solyc07g061720	3.5209066	3.100278522	323.7440701	2.22E-72	3.35E-69	Gibberellin 2-oxidase
Solyc02g086820	3.337479217	6.877234659	801.4773108	2.58E-176	3.90E-172	Carbonic anhydrase
Solyc02g070990	2.189725334	6.584749008	187.3276974	1.22E-42	5.27E-40	Chlorophyll a/b binding protein
Solyc05g014120	2.005530893	3.133249884	147.6399777	5.69E-34	1.46E-31	Os08g0119500 protein (Fragment)
Solyc12g099930	1.873780431	4.92924797	293.3348494	9.33E-66	1.09E-62	Serine-glyoxylate aminotransferase
Solyc12g094640	1.87018155	4.574741601	312.1172692	7.55E-70	9.52E-67	Glyceraldehyde-3-phosphate dehydrogenase B
Solyc05g045670	1.865668553	2.325244291	77.0066302	1.70E-18	1.19E-16	Glucose-6-phosphate/phosphate translocator 2
Solyc11g012590	1.846131838	3.099751394	181.1023165	2.78E-41	1.11E-38	UPF0497 membrane protein 12
Solyc04g074890	1.843153698	2.028946396	105.1871396	1.11E-24	1.40E-22	Unknown Protein
Solyc02g070980	1.835096298	8.436639195	192.5484509	8.83E-44	3.93E-41	Chlorophyll a/b binding protein

Table 2. Candidate Mutations for *tie1-1*. The Table lists all coding-region mutations on chromosome 2 between 20 and 45 megabases where the *tie1-1* alternate allele frequency was greater than 90% and where *tie1-1* and M82 differed in allele frequency by more than 60%.

Position on chromosome 2	Gene	Reference	Alternate	*tie1-1* depth	*tie1-1* percent alt	M82 depth	Heinz depth	Effect	Annotation
34001234	Solyc02g069570	C	T	33	93.94	46	47	Synonymous substitution	Pentatricopeptide repeat-containing protein
34091073	Solyc02g069670	C	A	76	90.79	68	45	Missense substitution	alpha-glucosidase
39010179	Solyc02g080120	G	T	11	100.00	29	46	Splice acceptor substitution	GA2-oxidsase 7/8

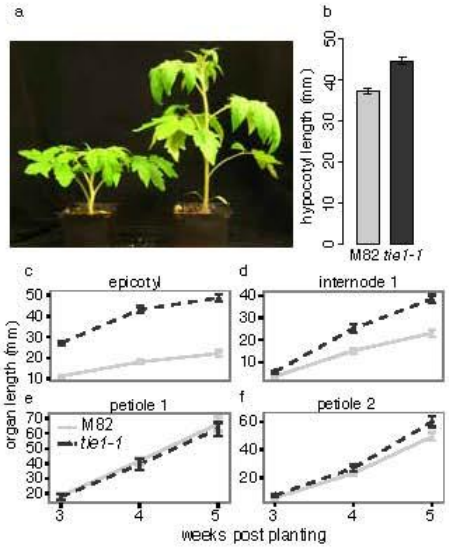

Figure 1. Growth phenotypes of *tie1-1* and M82.

Representative M82 (left) and *tie1*-1 (right) plants (a). Hypocotyl length (b) of 10 day old *tie1-1* and M82 seedlings grown on 0.5x MSMO and 0.7% agar in Phytatrays under long day (16:8) white light conditions in a growth chamber. n = >30 for each genotype. Length of epicotyl (c), internode 1 (d), petiole 1 (e), and petiole 2 (f) of three, four, and five week old *tie1-1* and M82 plants grown on soil in four-inch pots under long day (16:8) white light in a growth chamber. n = 8 for each genotype. The error bars show +/- SE.

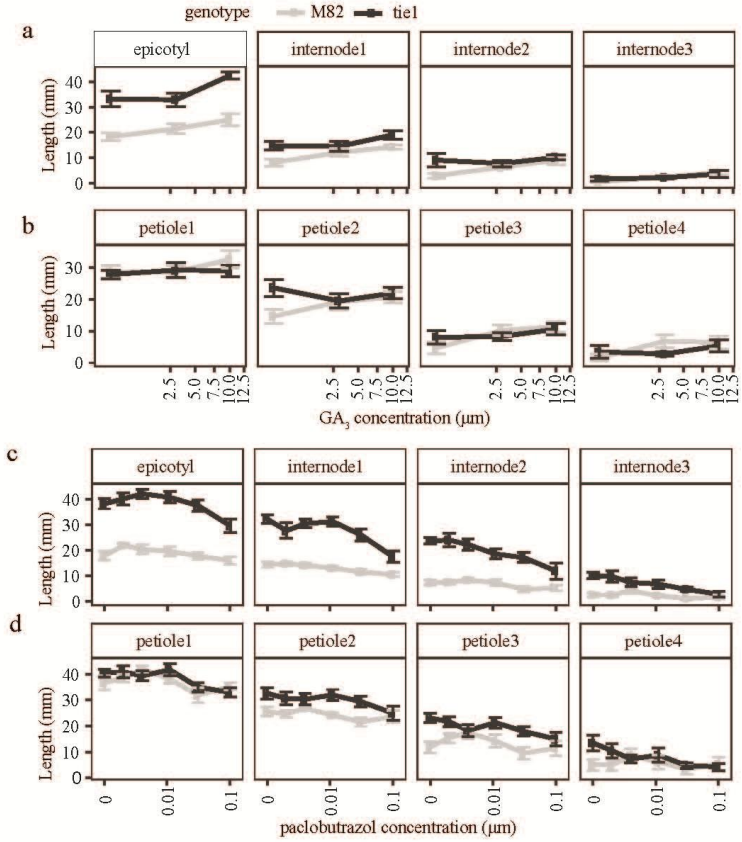

Figure 2. Response to application of bioactive GA_3 and GA biosynthetic inhibitor PAC. Internode length (a) and petiole length (b) of GA_3 treated *tie1-1* and M82 plants grown in 4-in pots in soil under long day white light conditions in a growth chamber. Plants were sprayed with 0 μM (mock), 3 μM, or 10 μM GA_3 every two days beginning two weeks after plating. Internode length (c) and petiole length (d) of PAC treated *tie1-1* and M82 plants grown in 4-in pots in soil under long day white light conditions in a growth chamber. Plants were watered with 0 μM (mock), 0.001 μM, 0.003 μM, 0.01 μM, 0.03 μM, or 0.1 μM every three days beginning two and a half weeks after plating.

Measurements for both treatments were taken four weeks after plating and n = 8 for each genotype, treatment, and concentration. Error bars represent +/- SE.

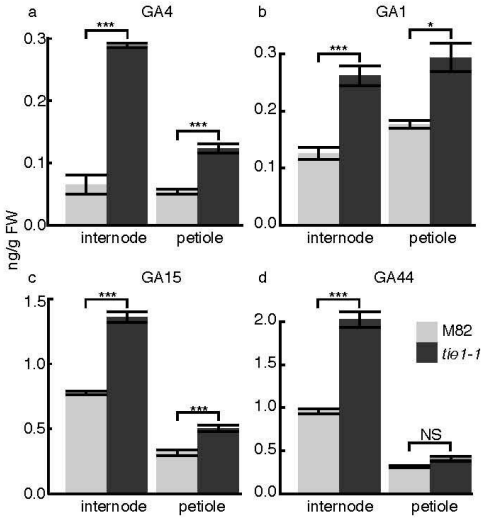

Figure 3. Endogenous concentration of various active and intermediate and GAs. Endogenous concentration of active GA_4(a) and GA_1 (b) and inactive intermediates GA_{15} (c) and GA_{44} (d) in the *tie1-1* mutant and M82 internodes and petioles. 100-200 mg FW was harvested from three and a half week old plants grown under long day white light conditions in a growth chamber. Nine plants contributed to each of three biological replicates for each organ or each genotype. Error bars represent +/- SE. *** $p < 0.001$, ** $p < 0.01$, * $p < 0.05$, NS = not significant.

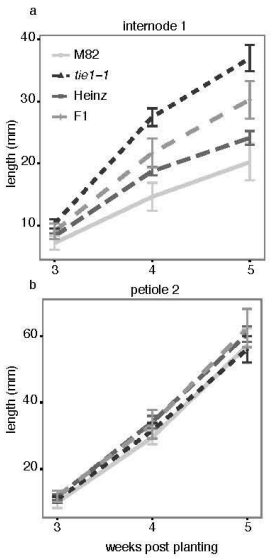

Figure 4. Growth phenotypes of the Heinz mapping parent, wildtype M82, *tie1-1* mutant, and F1 progeny of a Heinz x *tie-1* cross.

Internode 1 length (a) and petiole 2 length (b) of three, four, and five week old Heinz mapping parent, wildtype M82, *tie1-1* mutant, and F1 generation of a Heinz x *tie1-1* cross plants grown on soil in four-inch pots under long day (16:8) white light in a growth chamber. n = 8 for each genotype. The error bars show +/- SE.

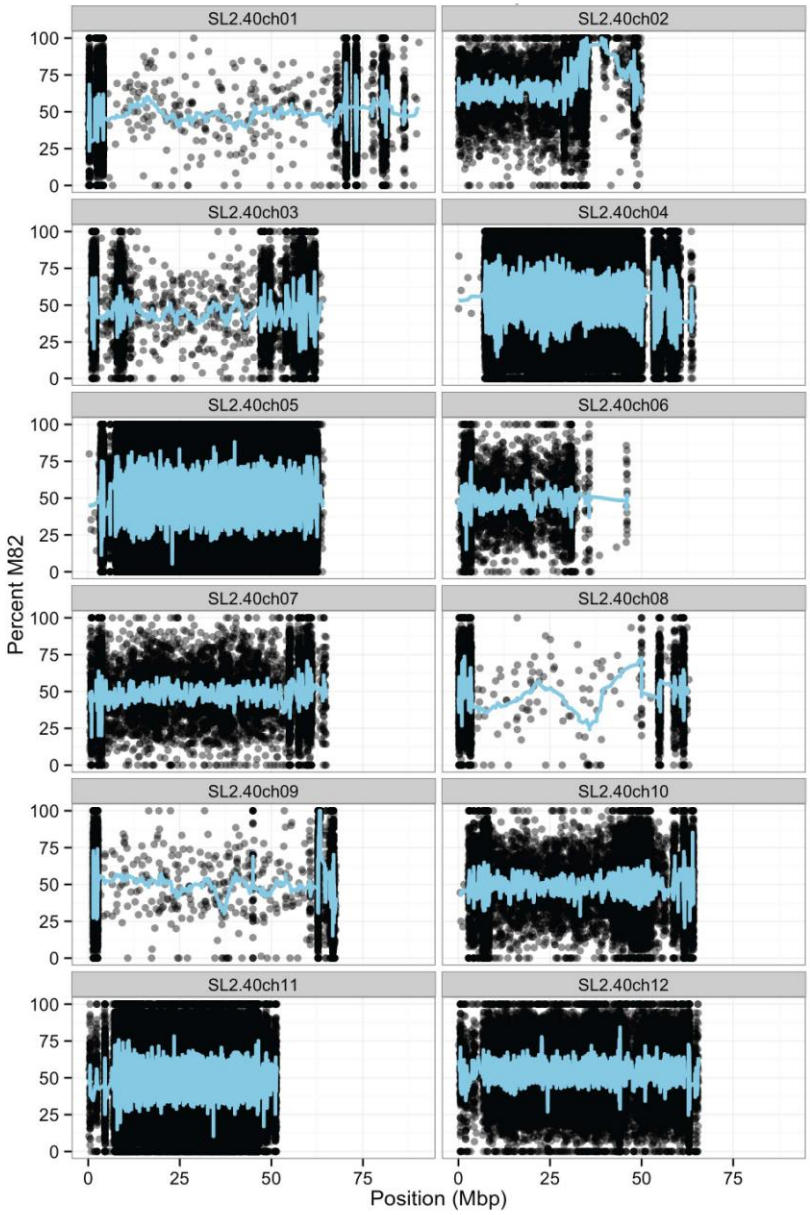

Figure 5. BSA reveals a peak on chromosome 2.

Each point represents a SNP segregating between M82 and Heinz in the *tie1-1* BSA pool. The y-axis indicates the percentage of reads that had the M82 genotype in the *tie1-1* BSA pool. The x-axis indicates the position along the chromosome in base pairs. The blue line shows a 20 SNP running average of M82 percentage.

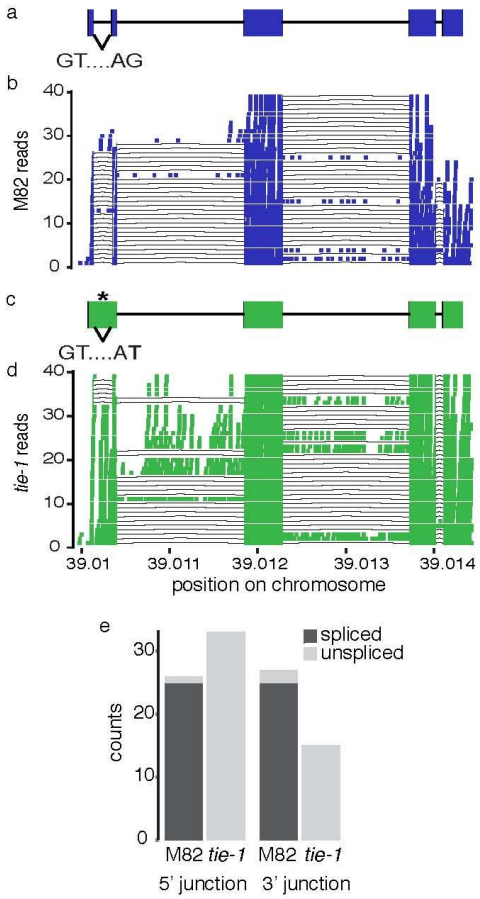

Figure 6. Gene model of the M82 and *tie1-1* GA2ox 7 and quantification of *tie1-1* intron retention.

(a) and (c): Schematic showing the wild-type and *tie1-1* gene structure (respectively) and the G->T splice acceptor base change. (b) and (d): Plot of M82 (B) and *tie1-1* (d) Illumina

RNAseq reads mapped to the Heinz genome. Thin lines connect splice junctions present in RNAseq reads and thick lines indicate alignment between an RNAseq read and the reference. Note the extensive retention of intron 1 in *tie1-1*. (e) Quantification of reads that are spliced or unspliced crossing the 5' or 3' intron 1 splice junction. The apparent intron splicing indicated by 6 reads in the *tie1-1* intron 1 (d) is actually due to read-misalignment by the mapping software and upon detailed inspection these reads do not represent intron 1 splicing.

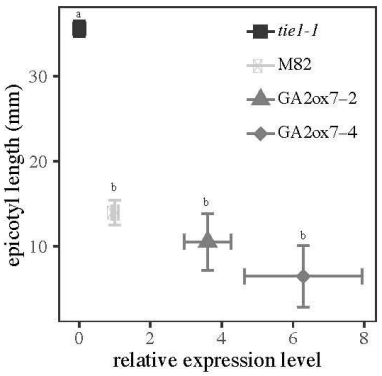

Figure 7. Full length *GA2ox7* (Solyc02g080120) complements the *tie1-1* phenotype. Gene expression of *GA2ox7* and epicotyl length of 4 week old M82, *tie1-1*, and two independent complementation lines. Plants were grown on soil in four-inch pots under long day (16:8) white light in a growth chamber. n > 5 for each genotype. The error bars show +/- SE.

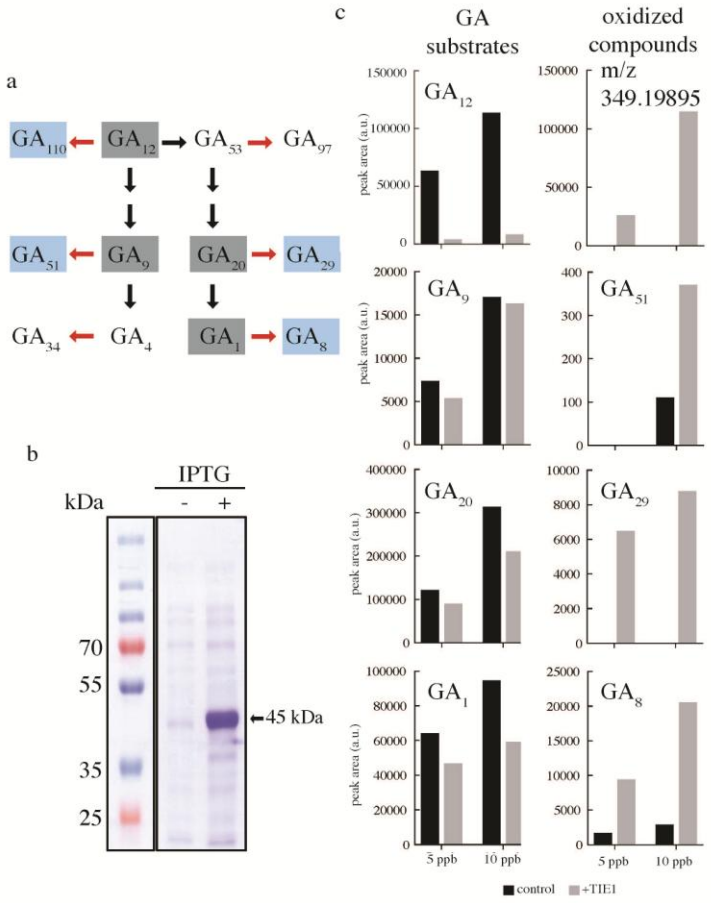

Figure 8. TIE catalyzes the oxidation of C_{19}- and C_{20}-GA molecules.

(a) Schematic representation of GA metabolism highlighting the GA molecules analyzed in the in vitro activity tests. Shaded in blue are the oxidized compounds. Red arrows indicate the reactions catalyzed by 2-oxidases. (b) Coomasie-stained gel showing the production of TIE-6xHis in *E. coli*. (c) Use of different GA molecules (left column) and production of their

oxidized versions (right column) by bacterial extracts containing TIE-6xHis induced or not at 37ºC for 2 h.. Exp 1 and Exp 2 are two biological replicates using 5 and 10 ppb, respectively, of GA12, GA9, GA20 and GA1. The most likely ion diagnostic for GA110 is that of m/z = 349.19895, but there is no standard available.